Alternative Methods in Spectral Factorization

A Modeling and Design Tool

D.A. Overdijk[‡], **N. van de Wouw**[*], **A. de Kraker**[*]

[‡] Eindhoven University of Technology,
Department of Mathematics and Computing Science,
P.O. Box 513, 5600 MB Eindhoven,
The Netherlands

[*] Eindhoven University of Technology,
Department of Mechanical Engineering,
P.O. Box 513, 5600 MB Eindhoven,
The Netherlands

Abstract

Spectral factorization can be used to recover the complex transfer function of a linear, causal, stable, minimum-phase system from merely its amplitude information. Two different approaches are presented, resulting in two consistent expressions for the complex transfer function. Firstly, an approach using Fourier theory is followed [Papoulis, 1977; Priestley, 1981]. Secondly, a new approach using potential theory results is presented. Spectral factorization can be successfully used as a modeling tool. Moreover, its capability to serve as a design tool is emphasized. These fields of application are illustrated by means of examples.

AMS subject classification: 93B30, 42A99, 31A99
Keywords: Spectral factorization, system identification, system design

1 Introduction

Let $H(s)$, $s \in \mathbb{C}$, be the Laplace transform of the impulse response $h(t)$, $t \in \mathbb{R}$, of a *causal and stable*, linear time-invariant system. Furthermore, the system satisfies the *minimum phase* property, i.e. the inverse system is causal and stable as well. So, a negative real number α exists such that $H(s)$ is analytic and has no zeros in the domain $G = \{s \in \mathbb{C} \mid \mathrm{Re}(s) > \alpha\}$. Let us introduce the function

$$A(\omega) := H(j\omega)H^*(j\omega) = \mid H(j\omega) \mid^2, \quad \omega \in \mathbb{R}, \tag{1}$$

where H^* is the complex conjugate of H. In the following sections we show that the transfer function $H(s)$ of a *causal and stable* system satisfying the *minimum-phase* property is uniquely determined by the value of $\arg(H(0))$ and the function $A(\omega)$ in (1) provided that $A(\omega)$ satisfies the Paley-Wiener condition

$$\int_{-\infty}^{\infty} \frac{\mid \ln A(\omega) \mid}{1+\omega^2}\, d\omega \neq \infty \tag{2}$$

We discuss two alternative constructions of $H(s)$, given the function $A(\omega)$ and $\arg(H(0))$. In section 2, we describe a construction using Fourier theory, whereas in section 3 a construction based on two-dimensional potential theory is presented. In section 4, the method of spectral factorization is applied to illustrate its aptitude as a modeling and design tool. Some conclusions are presented in section 5.

2 Construction of the transfer function H(s) using Fourier theory

Let us consider the function $W(s) := H'(s)/H(s)$, $s \in G$, which is analytic on the domain G. Hence, the function $V(s) := \int_0^s W(\xi)\, d\xi$, with contour in G, is also analytic on G. If we define $\hat{H}(s) := H(0)\frac{e^{V(s)}}{H(s)}$, $\hat{H}(s) = 1$ on G and, therefore,

$$H(s) = e^{V(s)+\ln|H(0)|+j\arg(H(0))} := e^{c(s)}, \quad s \in G, \tag{3}$$

with $c(s)$ analytic on G and unique modulo $2\pi j$. Furthermore, in view of (1),

$$A(\omega) = e^{2\mathrm{Re}(c(j\omega))} \text{ or } \mathrm{Re}(c(j\omega)) = \frac{1}{2}\ln(A(\omega)), \quad \omega \,\epsilon\, \mathbb{R}. \tag{4}$$

In view of (3) the problem to be solved consists of the construction of an analytic function $c(s)$ on G satisfying (4) and

$$\mathrm{Im}(c(0)) = \arg(H(0)). \tag{5}$$

We show that $c(s)$ on G is uniquely determined by (4) and (5) modulo $2\pi j$. As stated in the introduction, this is done in the present section using Fourier theory.

Hereto, we transform the complex s-plane into the complex z-plane using the Möbius transformation

$$z = \frac{1-s}{1+s} \;\; ; \;\; s = \frac{1-z}{1+z}. \tag{6}$$

The imaginary axis in the s-plane corresponds to the unit circle in the z-plane such that

$$s = j\omega \;\; \leftrightarrow z = e^{-2j\arctan(\omega)}, \;\; \omega \,\epsilon\, \mathbb{R} \;\; \text{and} \;\; z = e^{j\theta} \;\; \leftrightarrow s = -j\tan\frac{\theta}{2}, \;\; -\pi < \theta < \pi. \tag{7}$$

Furthermore, the half plane $\mathrm{Re}(s) > 0$ corresponds to the interior domain $\mid z \mid < 1$ of the unit circle. We translate the problem described in (4) and (5) from the s-plane to the z-plane as follows. Construct a function $C(z)$, which is analytic for $\mid z \mid < 1$, such that

$$r(\theta) := \mathrm{Re}(C(e^{j\theta})) = \frac{1}{2}\ln\left(A\left(\tan\frac{\theta}{2}\right)\right), \;\; -\pi < \theta < \pi, \;\; \text{and} \;\; \arg(H(0)) = \mathrm{Im}(C(1)). \tag{8}$$

The relation between $c(s)$ and $C(z)$ follows from (6) and (7):

$$\begin{aligned} &c(s) = C\left(\frac{1-s}{1+s}\right), \mathrm{Re}(s) > 0, \;\; C(z) = c\left(\frac{1-z}{1+z}\right), \mid z \mid < 1, \\ &c(j\omega) = C\left(e^{-2j\arctan(\omega)}\right), \omega \,\epsilon\, \mathbb{R}, \;\; \text{and} \;\; C(e^{j\theta}) = c\left(-j\tan\frac{\theta}{2}\right), -\pi < \theta < \pi. \end{aligned} \tag{9}$$

It follows from the Paley-Wiener condition (2) that $\int_{-\pi}^{\pi} \mid r(\theta) \mid d\theta = \int_{-\infty}^{\infty} \frac{|\ln A(\omega)|}{1+\omega^2}\, d\omega \neq \infty$. So, we can write $r(\theta)$ as a Fourier series: $r(\theta) = \sum_{n=-\infty}^{\infty} r_n\, e^{jn\theta}, \;\; -\pi < \theta < \pi$, where the Fourier coefficients $r_n, \; n = 0, \pm 1, \pm 2, \ldots$, are given by

$$r_n = \frac{1}{2\pi}\int_{-\pi}^{\pi} r(\theta) e^{-nj\theta} d\theta = \frac{1}{\pi}\int_{0}^{\pi} r(\theta)\cos(n\theta)\, d\theta, \tag{10}$$

since $r(\theta)$ is real and even. Hence, $r_n = r_{-n}\,\epsilon\,\mathbb{R}, \;\; n = 0, \pm 1, \pm 2, \ldots$. The function

$$C(z) = r_0 + 2\sum_{n=1}^{\infty} r_n\, z^n + j\arg(H(0)), \;\; \mid z \mid < 1, \tag{11}$$

is analytic for $\mid z \mid < 1$, and

$$\begin{aligned} \mathrm{Re}(C(e^{j\theta})) &= \frac{1}{2}\left[C(e^{j\theta}) + C^*(e^{j\theta})\right] \\ &= \frac{1}{2}\left[r_0 + 2\sum_{n=1}^{\infty} r_n\, e^{jn\theta} + r_0 + 2\sum_{n=1}^{\infty} r_n^*\, e^{-jn\theta}\right] = \sum_{n=-\infty}^{\infty} r_n\, e^{jn\theta} = r(\theta), \\ \mathrm{Im}(C(1)) &= \arg(H(0)). \end{aligned} \tag{12}$$

So, the function $C(z)$ in (11) satisfies (8) and therefore $C(z)$ is the unique solution of the problem described in (8).

We now summarize the result of this section. Use (3), (9) and (11) to conclude

$$H(s) = \exp\left(r_0 + 2\sum_{n=1}^{\infty} r_n \left(\frac{1-s}{1+s}\right)^n + j\arg(H(0))\right), \;\; \mathrm{Re}(s) > 0. \tag{13}$$

Use (7) and (13) to obtain

$$H(j\omega) = \exp\left(r_0 + 2\sum_{n=1}^{\infty} r_n e^{-2jn\arctan(\omega)} + j\arg(H(0)) \right), \quad \omega \,\epsilon\, \mathbb{R}. \tag{14}$$

Finally, from (8) and (10) we get

$$r_n = \frac{1}{2\pi} \int_0^{\pi} \ln\left(A\left(\tan\frac{\theta}{2} \right) \right) \cos(n\theta)\, d\theta, \tag{15}$$

for $n = 0, 1, 2, \ldots$. The numerical calculation of the coefficients r_n can be performed efficiently using a Fast-Fourier-Transform (FFT) algorithm.

3 Construction of the transfer function H(s) by methods from potential theory

In this section, we discuss an alternative construction of the transfer function $H(s)$ starting with the problem formulated in (4) and (5). Write $c(s) = c(x+jy) = u(x,y) + jv(x,y),\ (x,y)\,\epsilon\,\mathbb{R}^2$, where $u(x,y) = \mathrm{Re}(c(s))$ and $v(x,y) = \mathrm{Im}(c(s))$. According to (4) and (5) we have

$$u(0,y) = \frac{1}{2}\ln(A(y)), \quad y\,\epsilon\,\mathbb{R}, \quad \text{and} \quad v(0,0) = \arg(H(0)). \tag{16}$$

Since $c(s)$ is analytic for $\mathrm{Re}(s) > 0$, the function $u(x,y)$ is harmonic in the domain $D = \{(x,y)\,\epsilon\,\mathbb{R}^2 \mid x > 0\}$, i.e. u satisfies the two-dimensional potential (Laplace) equation on D [Schwartz et al., 1960]. The harmonic function u is given on the boundary of D, i.e. on the y-axis; see (16). Using Green's function, we can solve the Dirichlet problem to calculate the harmonic function u on D from its values on the boundary of D. From standard calculations we obtain

$$u(x,y) = -\int_{-\infty}^{\infty} u(0,\eta)\, \frac{\partial G_r}{\partial \xi}(0,\eta;x,y)\, d\eta, \ (x,y)\,\epsilon\, D. \tag{17}$$

Herein, Green's function $G_r(\xi,\eta;x,y)$ in the point (ξ,η) corresponding to the source point $(x,y)\,\epsilon\, D$ and vanishing on the boundary of D is given by

$$G_r(\xi,\eta;x,y) = \frac{1}{4\pi}\ln\left(\frac{(\xi-x)^2 + (\eta-y)^2}{(\xi+x)^2 + (\eta-y)^2} \right), \quad (x,y)\,\epsilon\, D. \tag{18}$$

From (16), (17) and (18) we get

$$u(x,y) = \frac{1}{2\pi}\int_{-\infty}^{\infty} \frac{x\ln(A(\eta))}{x^2 + (\eta-y)^2}\, d\eta, \quad (x,y)\,\epsilon\, D. \tag{19}$$

It follows from the Paley-Wiener condition (2) that the integral in (19) converges for all $(x,y)\,\epsilon\, D$. Using the Cauchy-Riemann differential equations to calculate $v(x,y) = \mathrm{Im}(c(s))$ from $u(x,y) = \mathrm{Re}(c(s))$, we obtain

$$v(x,y) = \frac{1}{2\pi}\int_{-\infty}^{\infty} \frac{(\eta-y)\ln(A(\eta))}{x^2 + (\eta-y)^2}\, d\eta + \beta, \quad (x,y)\,\epsilon\, D, \tag{20}$$

in which β follows from (16), i.e. $\beta = \arg(H(0))$. Using elementary calculations, we conclude that $c(s) = c(x+jy)$ can be expressed as

$$c(s) = \frac{1}{2\pi}\int_{-\infty}^{\infty} \left(\frac{\ln(A(x\eta+y))}{1+\eta^2} + \frac{j\eta}{x^2+\eta^2}\ln\left(\frac{A(y+\eta)}{A(y-\eta)} \right) \right) d\eta + j\arg(H(0)), \quad (x,y)\,\epsilon\, D. \tag{21}$$

From (3) and (21) we conclude

$$H(j\omega) = e^{c(j\omega)} = \sqrt{A(\omega)}\exp\left(\frac{j}{2\pi}\int_0^{\infty} \frac{1}{\eta}\ln\left(\frac{A(\omega+\eta)}{A(\omega-\eta)} \right) d\eta + j\arg(H(0)) \right), \quad \omega\,\epsilon\,\mathbb{R}. \tag{22}$$

4 Applications

In this section, two applications of the spectral factorization method will be presented. The first application will mainly illuminate the modeling potential of the method. The second application will illustrate its suitability to tackle design-related problems.

It should be noted that the input data for the spectral factorization method concern the amplitude of the transfer function. In practice, these data, originating from experiments or numerical simulations, will mostly have a limited level of accuracy due to statistical, numerical or measurement errors. In the following examples, however, the amplitude data will be taken from an existing, exact, analytical model. This enables us to isolate the numerical error that the spectral factorization algorithm introduces in its application as a modeling tool. In the construction of the transfer function using Fourier theory (see section 2), these errors are due to, firstly, the limited accuracy of the FFT-algorithm that is used to compute the coefficients r_n in (15) and, secondly, the finite approximation of the sum in (14). When applying the construction based on potential theory results, the error stems from the numerical approximation of the integral in (22). The first example will show that these errors can be ensured to be very small. In general, the errors in the available amplitude data will be significantly larger than the numerical errors introduced by the factorization algorithm. Furthermore, data concerning the amplitude of the transfer function will generally (at least in modeling applications) be available only up to a certain frequency ω_{max}. However, the spectral factorization method requires data up to very high frequencies (theoretically up to infinitely high frequencies). Consequently, amplitude data will have to be generated artificially for $\omega > \omega_{max}$. In general, the order of the transfer function can be estimated from the data for $\omega < \omega_{max}$. For $\omega > \omega_{max}$ the former data can be supplemented with data following the correct order. It should be noted that use of the correct order is crucial with respect to the accuracy of the spectral factorization estimate. In the following examples, however, exact amplitude information is available up to infinite frequencies. The actual results of the following examples are computed using the method described in section 3. Application of the algorithm based on Fourier theory leads to completely consistent results.

In the first example, a single-degree-of-freedom, linear, causal, stable, minimum-phase system is considered with the frequency response function $H(j\omega)$ depending upon the angular frequency ω as follows: $H_v(j\omega) = \left({\omega_n}^2 - \omega^2 + 2j\zeta\omega_n\omega\right)^{-1}$. Here, ω_n is the undamped eigenfrequency and ζ is the dimensionless, viscous damping coefficient. The amplitude information used in the spectral factorization algorithm is given by $A_v(\omega) = \mid H_v(j\omega) \mid^2$. Using data taken from $A_v(\omega)$, the spectral factorization algorithm is applied using a convergence criterion for the computation of the integral in (22). This results in an estimate $\hat{H}_v(j\omega)$ for the transfer function. In figure 1 both $H_v(j\omega)$ and $\hat{H}_v(j\omega)$ are depicted in a Nyquist plot for discrete ω values. Figure 2 shows that the error $\mid \hat{H}_v(j\omega) - H_v(j\omega) \mid$ is very small and confirms the high quality of the spectral factorization estimate $\hat{H}_v(j\omega)$. Moreover, the error, displayed in figure 2, can be reduced even further when more numerical effort is done to estimate the integral in (22) with higher accuracy. This example clearly illustrates the modeling qualities of the spectral factorization method. It should be noted that, in the application of (22), the error $\mid \hat{H}_v(j\omega) \mid - \mid H_v(j\omega) \mid$ is absent by nature of the reconstruction.

In the second example, the viscous damping (of the first example) is replaced by hysteretic damping. The transfer function is then given by $H_h(j\omega) = \left({\omega_n}^2 - \omega^2 + jh_d\right)^{-1}$. Crandall [1997] has shown that this system is non-causal; the response anticipates the excitation. It is, therefore, clear that the complex transfer function

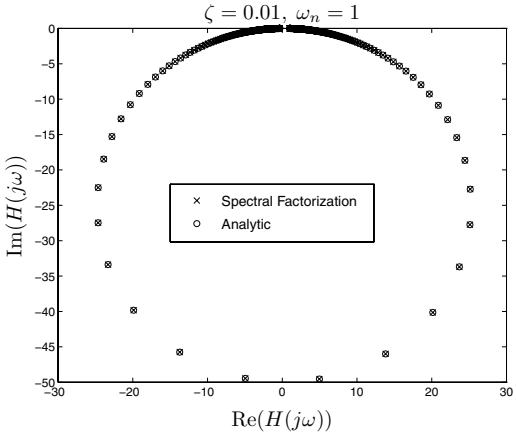

Figure 1: Comparison of $\hat{H}_v(j\omega)$ and $H_v(j\omega)$ in a Nyquist plot.

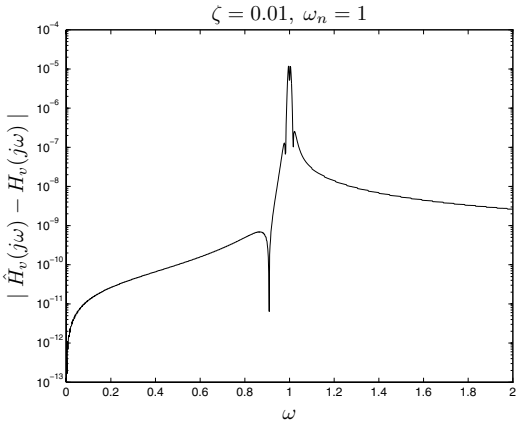

Figure 2: The error $\mid \hat{H}_v(j\omega) - H_v(j\omega) \mid$.

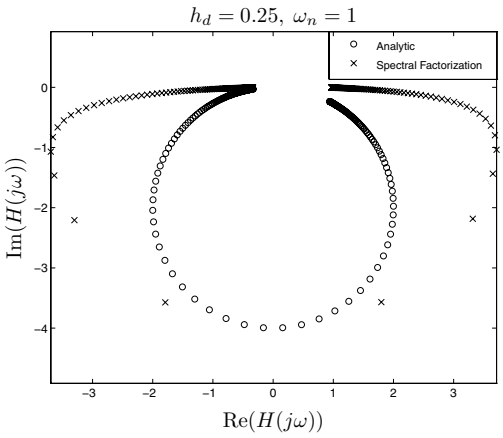

Figure 3: Comparison of $\hat{H}_h(j\omega)$ and $H_h(j\omega)$ in a Nyquist plot.

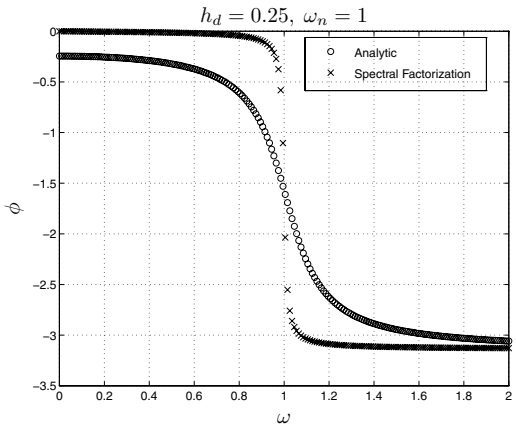

Figure 4: Comparison of phase of $\hat{H}_h(j\omega)$ and $H_h(j\omega)$.

$\hat{H}_h(j\omega)$, produced by the spectral factorization algorithm, will absolutely not resemble $H_h(j\omega)$, since $\hat{H}_h(j\omega)$ represents a causal system. So, here spectral factorization is not used as modeling technique but as a tool to design a linear, stable, causal, minimum-phase system that is *identical* to $H_h(j\omega)$ as far as the *amplitude* is concerned. Figure 3 shows both $H_h(j\omega)$ and $\hat{H}_h(j\omega)$ in a Nyquist plot and clearly visualizes the difference between these frequency response functions. Since the difference is merely a matter of phase, figure 4 depicts the phase ϕ of both frequency response functions. Of course, figures 3 and 4 raise interesting questions towards explaining the actual difference between $H_h(\omega)$ and $\hat{H}_h(\omega)$. However, these questions lie beyond the scope of this paper.

5 Conclusions

This paper gives a thorough and detailed description and evaluation of the spectral factorization method. Its ability to recover the complex transfer function of a linear causal, stable, minimum-phase system (including phase information) from merely amplitude information is illuminated.

Two different expressions concerning this transfer function are derived. Firstly, a solution path using Fourier theory is followed. Secondly, a new approach, using potential theory results, is introduced. These two results are found to be consistent when applying their resulting expressions.

Furthermore, it needs to be stressed that the possible applications are twofold. Firstly, spectral factorization can be used as a modeling tool; namely, the complex transfer function of an existing system can be recovered given input and output auto power spectra. Secondly, it can be successfully used as a tool to design a linear, causal, stable, minimum-phase system given the desired spectral characteristics of the system to be designed. Both fields of applications are illustrated by means of examples.

Moreover, it should be mentioned that the results can be forced to high levels of accuracy at rather low computational costs. Consequently, the accuracy of the result will generally not depend on the numerical errors of the spectral factorization algorithm, but the accuracy of the used amplitude information will be of major importance.

References

Crandall, S. (1997). Ideal hysteretic damping is non-causal. *ZAMM*, **77(9)**, 711–713.

Papoulis, A. (1977). *Signal analysis*. McGraw-Hill Book Company, New York.

Priestley, M. (1981). *Spectral analysis and time series, Volume 2:Multivariate series, prediction and control*. Academic Press, London.

Schwartz, M., Green, S., and Rutledge, W. (1960). *Vector Analysis*. Harper, New York.